# INTERLACED LINEAR ARRAYS FOR VIBRO-ACOUSTOGRAPHY: A NUMERICAL SIMULATION STUDY

**Glauber T. Silva†, James F. Greenleaf, and Mostafa Fatemi**
Mayo Clinic and Foundation, Rochester, MN, USA.
†Email: silva.glauber@mayo.edu

## Abstract

In this work, we study the beamforming of interlaced linear arrays for vibro-acoustography systems. The aim of this research is to model and design a system with a contact probe for *in vivo* applications. Two transducers with two identical linear arrays are studied: inline and fully interlaced arrays. The system point-spread function is given in terms of the dynamic ultrasound radiation force produced by the interference of the ultrasound beams generated by each array. A computer program simulates the beamforming of the arrays based on the spatial impulse method. Simulations using array parameters similar to conventional ultrasound systems present the resolution cells of both transducers focused at 50 mm of about $(1.2 \times 2.6 \times 18.0)$ mm in azimuth, elevation, and range. Sidelobes can be reduced to less than $-36$ dB through apodization. The interlaced arrays exhibit transverse resolution acceptable for medical imaging applications.

## Introduction

Vibro-acoustography is an imaging technique that produces a map (image) of the mechanical properties of an object by applying ultrasound dynamic radiation force on the object [1]. The radiation force is generated by two harmonic ultrasound focused beams driven at slightly different frequencies. The beams interfere in the focal region of the system producing a modulated ultrasound beam. The resulting beam generates the dynamic radiation force that has a component at the modulation frequency. This force causes the object (or region of interest) to vibrate emitting an acoustic field (*acoustic emission*) that can be detected by a hydrophone or microphone. The detected signal is used to synthesize an image of the object.

Clinical applications of ultrasound imaging systems require electronic beam focusing and steering. Linear array transducers are widely used for this purpose [2], because they can focus and steer the ultrasound beam laterally by electronically delaying the signals of the array elements. Linear array beamforming for vibro-acoustography shares similarities with its counterpart in conventional ultrasound (B-mode). The goals of beamforming for vibro-acoustography remain to achieve narrow beams with low sidelobes and minor effects of grating lobes.

An imaging system is characterized by its point-spread function (PSF). In vibro-acoustography, the PSF is given in terms of the dynamic radiation force at the modulation frequency. Thus, we shall call the vibro-acoustography PSF as the radiation force point-spread function (RFPSF). The dynamic radiation force depends, among other factors, on how the generated ultrasound beams overlap. This is related to the relative position of transducers that generate the beams. Consequently, the system resolution cell, defined as the volume enclosed by the RFPSF at $-12$ dB, depends on the relative position of the transducers.

Here, we study the beamforming of interlaced linear arrays for vibro-acoustography through numerical simulations based on the spatial impulse method [3]. Two transducers formed by two identical linear arrays are analyzed: inline and fully interlaced arrays. In the former, the elements of both arrays alternate along azimuth. In the latter, the alternation of the elements of both arrays take place in azimuth and elevation. In a recent work [4], transducers based on separated linear arrays were studied for vibro-acoustography applications. In these transducers, two linear arrays are placed side-by-side along azimuth (inline separated array) or elevation (parallel separated array). One advantage of interlaced over separated arrays is that in the former the array elements spans the entire transducer aperture. Results show that the resolution cell of both interlaced arrays focused at 50 mm is about $(1.2 \times 2.6 \times 18.0)$ mm in azimuth, elevation, and range. Sidelobes are reduced to less than $-36$ dB through apodization. The transverse resolution of the interlaced arrays are acceptable for medical imaging applications. The superiority of interlaced over separated arrays in vibro-acoustography is discussed.

## Theory

### *Dynamic ultrasound radiation force*

Consider two collimated ultrasound beams with frequencies $\omega_a = \omega_0$ and $\omega_b = \omega_0 + \Delta\omega$ propagating in an ideal fluid. The quantities $\omega_0$ and $\Delta\omega$ are the center and the difference frequencies, respectively. In vibro-acoustography applications $\Delta\omega/\omega_0 \ll 1$. The beams overlap in a region of the space which is defined as the focal zone of the system. This is referred here as dual beam mode (see Fig. 1). The resulting beam in the focal zone is a modulated ultrasound wave that is described

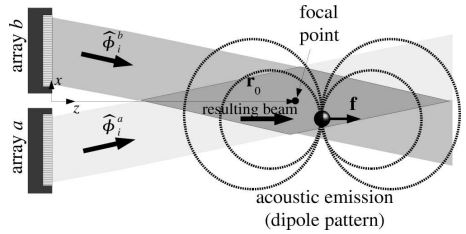


Figure 1: Dual beam mode.

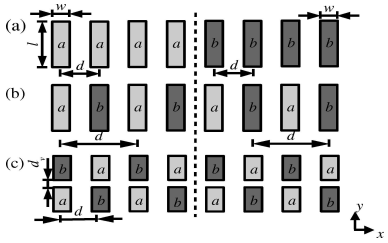


Figure 2: Linear array transducers.

by the following acoustic potential:

$$\phi_i(\mathbf{r},t) = \hat{\phi}_i^{(a)}(\mathbf{r}|\mathbf{r_0})e^{j\omega_a t} + \hat{\phi}_i^{(b)}(\mathbf{r}|\mathbf{r_0})e^{j\omega_b t}, \quad (1)$$

where $j$ is the imaginary unit, $\hat{\phi}_i^{(a)}$ and $\hat{\phi}_i^{(b)}$ are the complex amplitude functions, and $\mathbf{r}_0$ is the focal point of the system. Assume that a point-target is placed somewhere within or in the neighborhood of the system focal zone. The total (incident + scattered) pressure and velocity fields are denoted by $p$ and $\mathbf{v}$, respectively.

The radiation force exerted on the point-target by the incident modulated ultrasound wave is given by [5]

$$\mathbf{f} = \oint_S \langle \mathcal{L}\mathbf{n} - \rho_0 (\mathbf{v}\cdot\mathbf{n})\,\mathbf{v}\rangle\, dS, \quad (2)$$

where $S$ is a surface enclosing the object, the brackets $\langle\rangle$ denote average in time over a long time interval, the symbol $\cdot$ is the dot-product, $\mathcal{L} = \frac{\rho_0(\mathbf{v}\cdot\mathbf{v})}{2} - \frac{p^2}{2\rho_0 c_0^2}$ is the Lagrangian density of the total wave, and $\mathbf{n}$ is the unit normal vector of $S$ pointing inward. The modulated ultrasound beam (1) produces a harmonic force at the difference frequency. To separate this component in the radiation force, we define the short-term time average of a given function $s(t)$ at a time $t$ in an interval $T$ as $\langle s\rangle_T \equiv \frac{1}{T}\int_{t-T/2}^{t+T/2} s(\tau)d\tau$. Hence, Eq. (2) should be calculated using the short-term time average with the condition $2\pi/\omega_0 \ll T \ll 4\pi/\Delta\omega$. It is possible to show that for a ultrasound traveling wave the main contribution to the radiation force on a small spherical target comes from the scattered wave [6]. By following this hypothesis, one can show that the dynamic radiation force on the point-target at the difference frequency $\Delta\omega$ is given by [7]

$$\mathbf{f} = A_0\nabla[\hat{\phi}_i^{(a)}\hat{\phi}_i^{(b)*}]e^{j\Delta\omega t}, \quad (3)$$

where $A_0$ is a constant, $\nabla$ is the gradient operator, and * means the conjugate of a complex quantity. The radiation force on the point-target can be decomposed into axial and transverse components. The axial component lays on the direction of propagation of the ultrasound modulated beam. The transverse component is perpendicular to the axial component.

*Radiation force point-spread function (RFPSF)*

The vibro-acoustography PSF, here called radiation force point-spread function (RFPSF), is based on the acoustic emission of a point-target which is proportional to the radiation force on it. If we consider the point-target as a hard object attached to some sort of restoration force mechanism such as a small steel sphere suspended by a wire, we can approximate the acoustic emission of the point-target to a dipole radiation pattern. In this model, the normalized RFPSF is defined in terms of the dynamic ultrasound radiation force as follows

$$h_{\text{psf}}(\mathbf{r}|\mathbf{r}_0) \equiv \frac{\hat{f}(\mathbf{r}|\mathbf{r}_0)}{\hat{f}(\mathbf{r}_0|\mathbf{r}_0)}, \quad (4)$$

where $\mathbf{r}_0$ is the system focal point and $\hat{f}$ is the magnitude of the radiation force vector given in Eq. (3). Note that the RFPSF is a three-dimensional complex function, therefore, both phase and modulus of this function can be used to produce vibro-acoustographic images. Inasmuch as the modulated ultrasound beam in (1) depends upon the focal point $\mathbf{r}_0$, so does the RFPSF. This means that a vibro-acoustography system is only shift-invariant in the neighborhood of the system focal point. Changing the focal point usually modifies the system resolution cell.

*Linear arrays*

The beam produced by a linear array can be laterally steered by an angle $\theta_0$ and focused at different distances $r_0$ in the azimuth plane (plane normal to the linear array). A linear array consists of $N$ rectangular elements of width $w$ and height $l$ placed in a row with a constant interelement spacing $d$ (pitch). Consider a transducer with two linear arrays, $a$ and $b$, for a vibro-acoustography system. Each linear array has $N$ elements. The elements of the arrays are driven by two harmonic signals with proper phase values to focus and steer the resulting ultrasound beam. Fig. 2 shows the following transducers: (a) inline separated, (b) inline interlaced, and (c) fully interlaced arrays. To calculate the acoustic potential generated by the linear arrays described in Fig. 2, we use the spatial impulse method.

Table 1: Parameters used in the computer simulations.

| **Parameters** | **Values** |
|---|---|
| elements $(N)$ | 64 (inline), 128 (fully) |
| width $(w)$ | 0.15 mm |
| height $(l)$ | 12, 6 mm |
| pitch $(d)$ | 0.2, 0.4 mm |
| focus in elevation | 50 mm |
| ultrasound frequency $(f_0)$ | 3 MHz |
| speed of sound $(c_0)$ | 1480 m/s |

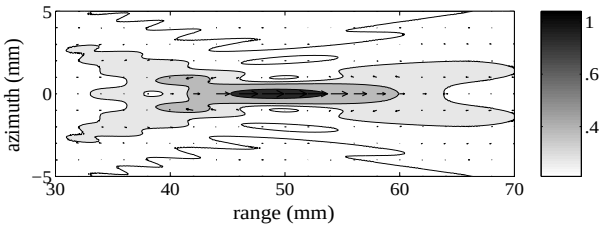


Figure 3: Ultrasound radiation force produced by the interlaced transducers. The arrows represent the direction of the force.

In this method, the acoustic potential generated by a flat piston is given as the time convolution between the spatial impulse function $h(\mathbf{r}, t)$ and the normal particle velocity $v_n(t)$ at the surface of the piston as follows:

$$\phi(\mathbf{r}, t) = v_n(t) \underset{t}{\star} h(\mathbf{r}, t). \tag{5}$$

To compute the function $h(\mathbf{r}, t)$ of rectangular pistons (array elements), we use the exact solution obtained by Emeterio *et al.* [8]. For the sake of simplicity, we omit the mathematical expressions of $h(\mathbf{r}, t)$ here. A program, written in C programming language, was used to compute Eq. (4) by using Eqs. (3) and (5). The parameters used in the simulations can be seen in Table 1.

**Results**

Simulations have shown that the main contribution for the RFPSF comes from the axial component of the radiation force. The transverse component of the force contributes with less than 10% of the axial component. Fig. 3 shows the radiation force produced by the interlaced arrays in the azimuth plane.

The shape of the resolution cell is subject to distortions as the ultrasound beam is steered and focused at different points in the medium. We define the relative broadening of the resolution cell as $\Delta\eta \equiv (1 - \eta_1/\eta_2) \times 100\%$, where is $\eta_i$ is the cell width along range, azimuth, or elevation. The ultrasound beam is focused at the position $i = 1, 2$ specified by $r_0 = 30, 70$ mm, respectively. Fig. 4 shows contour plots of the RFPSF in the azimuth plane. The relative broadening of the resolution cell along range for all transducer is

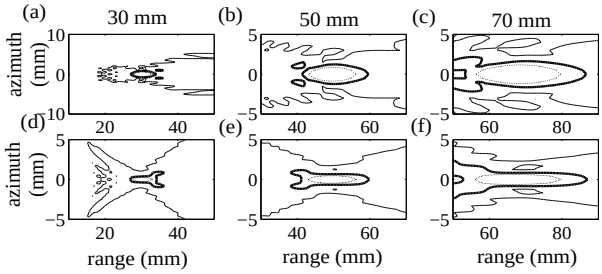


Figure 4: RFPSF in the azimuth plane. (a-c) Inline separated array. (d-f) Interlaced arrays. **Legend**: solid line $-30$ dB, thick line $-12$ dB, and dotted line $-6$ dB.

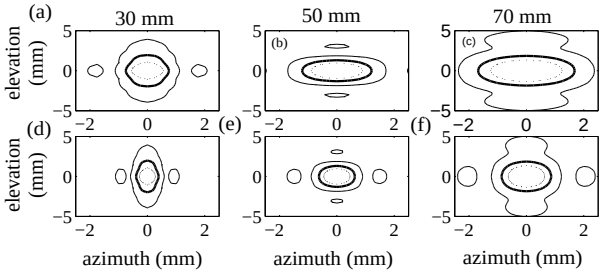


Figure 5: RFPSF in the focal plane. (a-c) Inline separated array. (d-f) Interlaced arrays. **Legend**: solid line $-30$ dB, thick line $-12$ dB, and dotted line $-6$ dB.

$\Delta\eta = 78.2\%$. Fig. 5 shows contour plots of the RFPSF in the focal plane. In azimuth, the relative broadening of interlaced arrays is $\Delta\eta = 54.3\%$, while for the inline separated array is $\Delta\eta = 55.4\%$. In elevation, all transducers have $\Delta\eta = -11.1\%$. When the focal point is at $r_0 = 50$ mm the resolution cell of the interlaced arrays is $(1.2 \times 2.6 \times 18)$ mm in azimuth, elevation, and range. The inline separated array has the azimuthal resolution two times larger than the interlaced arrays.

Fig. 6 shows the RFPSF of the interlaced arrays, in which each individual array was apodized by the Bartlett's function

$$a_n = 1 - \left| \frac{2x^{(n)}}{D} \right|, \tag{6}$$

where $x_n$ is the center of the $n^{\text{th}}$-array element and $D = 25.6$ mm is the transducer lateral aperture. After the apodization, sidelobe levels of the RFPSF are as low as $-36.0$ dB and mainlobe is $5$ dB lower than the non-apodized RFPSF. Furthermore, the RFPSF mainlobe width at $-12$ dB became 12% wider.

The inline interlaced array exhibits grating lobes because its array pitch ($d = 0.4$ mm) is larger than half of the ultrasound wavelength ($0.5$ mm). Fig. 7 shows grating lobes in the RFPSF of the inline interlaced array. When the beam is steered from $0^{\text{o}}$ to $-40^{\text{o}}$ the grating lobe level increases from $-36.4$ dB to $-4.4$ dB.

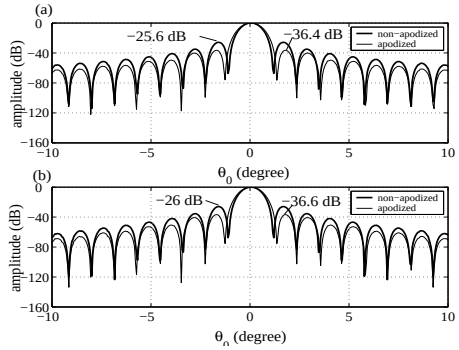


Figure 6: Apodization of the RFPSF: (a) inline and (b) fully interlaced arrays.

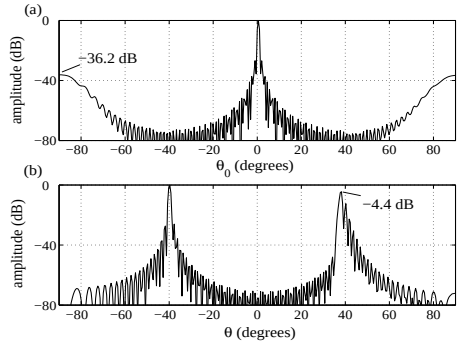


Figure 7: Grating lobe produced by the inline interlaced array.

## Summary

We have presented a study of interlaced linear arrays for vibro-acoustography. The contribution of the transverse radiation force to the RFPSF is small (less than 10%). However, the effects of this component on the images is unknown. The interlaced arrays have a better resolution compared to the separated inline array. Even though not shown here, this result is also true when we compare interlaced with the parallel separated array. The RFPSF of all array arrangements exhibited a high relative broadening $\Delta\eta = 78.2\%$ in range when the beam is focused from 30 to 70 mm. The variations of the RFPSF could be reduced if the transducer aperture varied as a function of the focus position. The RFPSF of the interlaced arrays are very similar except for grating lobes produced by the inline interlaced array. Because of this, the inline interlaced array could be used as a switched linear array, which operates without beam steering. Sidelobes in the RFPSF were reduced to as low as $-36$ dB through apodization. In conclusion, the transversal resolution of interlaced arrays $(1.2 \times 2.6)$ mm in azimuth and elevation is acceptable for medical imaging applications.

## Acknowledgments

This work was partially supported by NIH-grant EB00535-01.

## References

[1] Mostafa Fatemi and James F. Greenleaf. Ultrasound-stimulated vibro-acoustic spectrography. *Science*, 280:82–85, 1998.

[2] Peter N. T. Wells. Ultrasonic imaging of the human body. *Report on Progress of Physics*, 62:671–722, 1999.

[3] Peter R. Stephanishen. Transient radiation from pistons in a rigid infinity planar baffle. *Journal of the Acoustical Society of America*, 49:1627–1638, 1971.

[4] Glauber T. Silva and Mostafa Fatemi. Linear array transducers for vibro-acoustography. In *IEEE Ultrasonics Symposium Proceedings*, pages 611–613, Munich, Germany, October 2002. IEEE Ultrasonics, Ferroeletrics, and Frequency Control.

[5] K. Beissner. The acoustic radiation force in lossless fluids in eulerian and lagrangian coordinates. *Journal of the Acoustical Society of America*, 103(5):2321–2332, May 1998.

[6] L. P. Gor'kov. On the forces acting on a small particle in an acoustical field in an ideal fluid. *Soviet Physics - Doklady*, 6(9):773–775, March 1962.

[7] Glauber T. Silva. *Image Formation in Vibro-acoustography*. PhD thesis, Universidade Federal de Pernambuco, Centro de Informática, 2003.

[8] Jose Luis San Emeterio and Luis G. Ullate. Diffraction impulse response of rectangular transducers. *Journal of the Acoustical Society of America*, 92(2):651–662, August 1992.